RSC Advances

ROYAL SOCIETY OF CHEMISTRY

www.rsc.org/advances

Development of asymmetrical near infrared squaraines with large Stokes shift

Xiaoqian Liu[1], Bokun Cho[3], Liyan Chan[1], Wei Lei Kwan[2],Chi-Lik Ken Lee[1]**

[1]Centre for Biomedical and Life Sciences, Department of Technology, Innovation and Enterprise (TIE), Singapore Polytechnic, Singapore. [2]Engineering Product Development, Singapore University of Technology and Design, Singapore. [3]Energetics Research Institute (EnRI), Nanyang Technological University, Singapore.

Corresponding authors: Wei Lek Kwan (kwanwl@sutd.edu.sg) and Chi-Lik Ken Lee (kenlee@sp.edu.sg).

Abstract

A new strategy of obtaining large Stokes shift squaraine dyes is reported. Archetypal near infrared squaraines typically have very sharp absorption peaks and small Stokes shifts due to their very rigid ground and excited state molecular structures. TDDFT calculations revealed that large Stokes shift in squaraines can be reached by structural relaxation of the excited state. We achieved Stokes shifts of 90nm by introducing a dibutyl- aniline side group and an electron withdrawing dicyano group to the squarate core. Wavefunction analysis indicates that that steric interactions and mesomeric effects in the ground and excited states of squaraines are crucial in determining the Stokes shift of the dye.

1. Introduction

In the last decade, there have been increasing interests in organic dyes, especially near infrared (NIR) dyes for diverse applications in light emitting diodes, field-effect transistors, organic photovoltaics, NIR-fluorescence imaging and photo dynamic therapy.[1-2] Their most notable features include strong absorption in the NIR region, tunable solubility in different solvents, and remarkable chemical and photostability. Great efforts have been made to develop more effective NIR dyes, including borondipyrromethenes (BODIPYs), pyrrolopyrrole cyanine and squaraines. [3] Among these fluorophores, squaraine compounds are actively being investigated as high performance components with resonance stabilized zwitterionic structures. [4]

Symmetric squaraines are the condensation products of one equivalent of squaric acid and two equivalents of suitable electron rich precursors. [5] These dyes possess effective absorption in NIR region (> 600 nm), narrow excitation and emission peaks with large molar extinction coefficients and quantum yields. [6] However, compared to these popular and intensely studied "classical" squaraines, asymmetric derivatives are considerably less investigated. Asymmetrical squaraines in donor-acceptor-donor (D-A-D) types can provide unidirectional flow of electrons, which may affect charge transfer in the molecule, resulting in the change of the physical properties and improvement in the performance of organic solar cells and dye sensitized solar cells. [7] More importantly, the structures

with one site of functional group like – COOH can provide mono specific binding site to some bio-molecules, such as: oligonucleotides, which will act as probes for multiple detection applications. [8]

Large Stokes shift is desirable in fluorescent labeling applications of dyes, as it reduces self-quenching effects and interference from excitation source. However, despite the favorable characteristics of squaraines, the Stokes shifts are typically 20-30 nm, which limits its potential applications.

Recently, asymmetrical squaraine dyes with large Stokes shifts (~90nm) has been reported. [2i, 3k] Shafeekh et. al. has shown that the large Stokes shifts in their squaraines are due to the dipole moment inversion of the excited state and its interaction with the solvent. [3k] Since the effect is due to the redistribution of the charge density between the excited and ground states, it is highly sensitive to the local environment.

Archetypal near infrared squaraines have very rigid ground and excited state structures due to their large conjugated systems. As a result, squaraines typically have very sharp absorption peaks and small Stokes shifts. In this paper, we explore an alternative approach to increase the Stokes shift in squaraines by stabilizing the excited state through structural relaxation. We achieved a large Stokes shift of 90nm by introducing a dibutyl-aniline side group and an electron withdrawing dicyano group to the squarate core. Wavefunction analysis indicates that steric interactions and mesomeric effects in the ground and excited states of squaraines is an important factor in determining the Stokes shift of the dye.

2. Results and Discussion

Asymmetrical squaraines can be synthesized through a variety of multi-step procedures using electron rich precursors. [9] In order to tune physical properties of asymmetrical squaraines, we choose a strategy that will facilitate structural diversification by first preparing semi-squariane salts and subsequently attaching various donor moieties. [10-13] Since squarylium dyes with tertiary arylamine groups are known to have better stability and solubility than those with heterocyclic end groups, and rotational relaxation is known the occur in the excited states of symmetrical arylamine-squaraines, [5d]

new asymmetrical squaraine dyes containing the substituted aniline are firstly developed (Scheme 1). [14]

The substituted aniline based semi-squaraine salt **1** is used as our first template and synthesized according to the steps reported in the literature. [15] Different substituted benzothiazolium quaternary iodides **2a-2c** are used in the reflux of 1-butanol and toluene (1:1) with salt **1** to achieve final product **3a-3c** in moderate yields. Notably, the halide functionality for **3b** and **3c** can serve as diversity point for further structure tuning and optimization. [16]
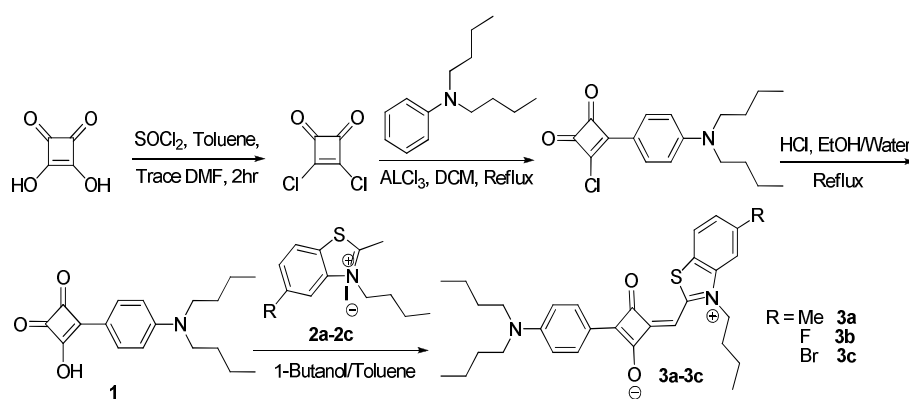
Scheme 1. Multi steps synthesis of squaraine **3a-c**.

To further investigate the influence on the structure difference of asymmetrical squaraines, another new series of compounds **6a-6c** are synthesized based on semi squaraine salt **4** which contains benzaothiazole moiety as a good electron donor and dicyanovinyl groups as a strong electron withdrawing group functionalized on the squarate core (Scheme 2). [17-19] A dicyanovinyl group is added in **6a**, in contrast to **3a,** to investigate the influence of additional acceptor functionalities at the squarate core. Compound **6b** and **6c** are also successfully prepared, respectively, to tune the conjugation size in the structure. The yields for **6a-6c** range from 8 % to 45%.
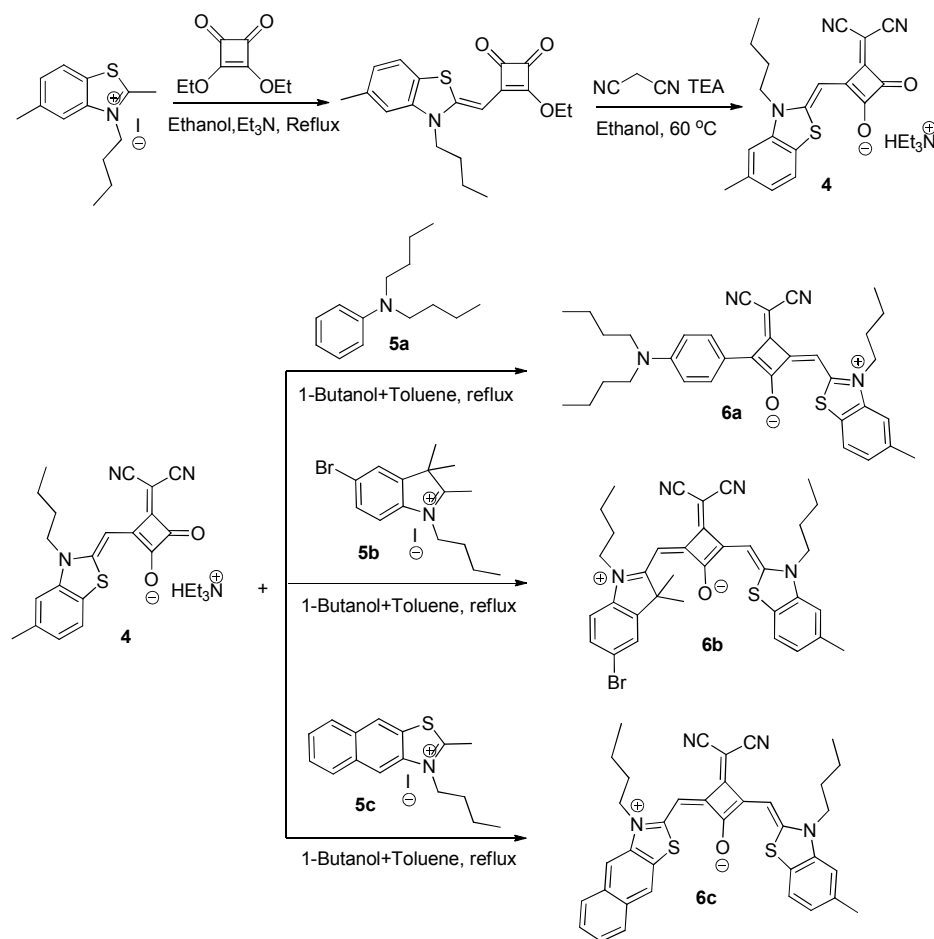
Scheme 2. Multi steps synthesis of squaraine **4, 6a-c**.

To gain insight into the relationship between molecular structure and physical properties, their absorption and fluorescence values are studied (Table 1; commercially available Cy5 and Cy5.5 standards were included for comparison).[18] All of them have shown strong absorptions in red visible to NIR regions with high molar absorption coefficients (ε) up to $10^4 \sim 10^5$ mol^{-1}cm^{-1}L in DMSO. The introduction of dicyanovinyl group on the squarate core (6a) resulted in significant red shift for the absorption wavelength and a larger stokes shift of 90 nm compared to 3a.

Table 1. Comparison of Squaraine dyes to Cy5 and Cy5.5 in DMSO.

Dyes[a]	.max(nm)	Δλ(nm)[b]	ΔE(eV)[c]	Δλ(nm)[d]	Ø[e]
3a	618	57	0.17	63	0.26
3b	618	57	0.17	--	0.22
3c	640	35	0.10	--	0.25
6a	**630**	**90**	**0.25**	**79**	**0.17**
Cy5	648	27	0.07	--	0.28
6b	680	32	0.08	37	0.21
6c	712	27	0.06	33	0.20
Cy5.5	685	35	0.08	--	0.23

[a]All the measurements were carried out in the concentration of 10 uM (or less) dyes which dissolve in DMSO. [b]Δλ (nm) = Stokes shift (nm) in experiments. [c]Stokes shift presents in ΔE(eV). [d]Δλ (nm) = Stokes shift (nm) in simulations. CAM-B3LYP/6-311+G(d,p) TDDFT calculations with DMSO PCM solvation (ωB97xD/6-31G(d) PCM optimized structures). [e]Ø = quantum yield.

Large Stokes shift in organic fluorophores has been attributed to intramolecular charge transfer (ICT) excitation state or local excitation (LE) with competing steric and mesomeric interactions. Both phenomena can cause a significant geometric difference between ground state and excited state, resulting in a large Stokes shift. The dibutyl aniline side chain of our squaraine dye is determined to be the deciding factor in causing a significant Stokes shift as both 3a and 6a has considerable larger Stokes shift than the other substrates despite scaffold similarity. Hence we will consider how both excitation mechanisms influence the N,N-dibutylaniline moiety during absorption and fluorescence.
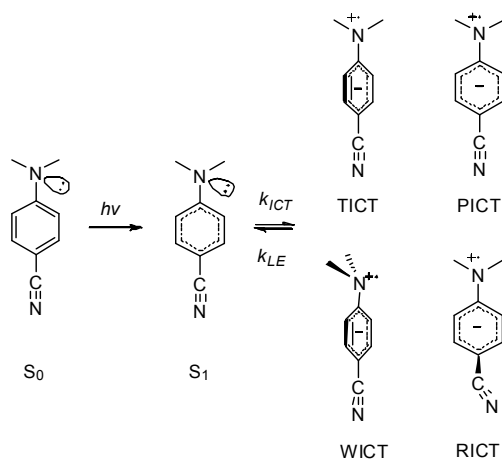
Figure 1. DMABN ground state, LE S_1 and possible ICT excited states

ICT generates a pseudo-zwitterionic excited state S_1 where a positive and negative charge resides at different regions of the fluorophore that stabilizes the charges respectively. This leads to a large structural change from the ground state S_0 resulting in the large Stokes shift. A well-documented example is 4,4-dimethylaminobenzonitrile[19] (DMABN, Figure 1.) and its para-alkylamine derivatives. Its close structural relation to our dibutyl aniline side chain makes its excitation mechanism plausible for our substrate. Several charge transfer states of DMABN and their kinetic and thermodynamic feasibility has been investigated theoretically. These includes the twisted ICT, TICT model[19b], where the amino group is in a perpendicular position relative to the benzene ring, the planar ICT, PICT[19c] which the amino group lies in the benzene plane, the wagged ICT, WICT[19d] which involves a rehybridization from planar sp2 to pyramidal sp3 of the amino nitrogen and lastly the rehybridized ICT, RICT[19d] involves a rehybridization of the cyano carbon atom from sp to sp2 entailing a bent cyano bond.

Table 2. Benchmarking of TDDFT methods for 3a, 6a, 6b and 6c in DMSO implicit solvation

Dye	TDDFT Method	Optimization Method	Solvation	λ_{abs}(nm)	λ_{em}(nm)	$\Delta\lambda$(nm)
3a	CAM-B3LYP/6-311+G(d,p)	ωB97x-D/6-31G(d)	SMD	520	598	78
	CAM-B3LYP/6-311+G(d,p)	**ωB97x-D/6-31G(d)**	**PCM**	**519**	**582**	**63**
	ωB97x-D /6-311+G(d,p)	ωB97x-D/6-31G(d)	SMD	511	596	85
	LC-BLYP/6-311+G(d,p)	ωB97x-D/6-31G(d)	SMD	480	600	120
	B3LYP/6-311+G(d,p)	ωB97x-D/6-31G(d)	SMD	572	606	34
	PBE0/6-31+G(d)	ωB97x-D/6-31G(d)	SMD	560	598	38
	CAM-B3LYP/6-311+G(d,p)	PBE0/6-31+G(d)	SMD	544	584	40
	PBE0/6-311+G(d,p)	PBE0/6-31+G(d)	SMD	570	594	24
	CAM-B3LYP/6-311+G(d,p)	CAM-B3LYP/6-31+G(d)	PCM	521	580	59
6a	CAM-B3LYP/6-311+G(d,p)	ωB97x-D/6-31G(d)	SMD	520	609	89
	CAM-B3LYP/6-311+G(d,p)	**ωB97x-D/6-31G(d)**	**PCM**	**528**	**606**	**78**
	ωB97x-D /6-311+G(d,p)	ωB97x-D/6-31G(d)	SMD	507	607	100
	LC-BLYP/6-311+G(d,p)	ωB97x-D/6-31G(d)	SMD	465	599	134
	B3LYP/6-311+G(d,p)	ωB97x-D/6-31G(d)	SMD	595	632	37
	PBE0/6-31+G(d)	ωB97x-D/6-31G(d)	SMD	579	623	43
	CAM-B3LYP/6-311+G(d,p)	PBE0/6-31+G(d)	SMD	589	620	31

	PBE0/6-311+G(d,p)	PBE0/6-31+G(d)	SMD	546	608	63
	CAM-B3LYP/6-311+G(d,p)	CAM-B3LYP/6-31+G(d)	PCM	531	606	75
6b	CAM-B3LYP/6-311+G(d,p)	ωB97x-D/6-31G(d)	SMD	576	614	39
	CAM-B3LYP/6-311+G(d,p)	**ωB97x-D/6-31G(d)**	**PCM**	**578**	**616**	**37**
	ωB97x-D /6-311+G(d,p)	ωB97x-D/6-31G(d)	SMD	572	613	41
	B3LYP/6-311+G(d,p)	ωB97x-D/6-31G(d)	SMD	604	634	30
	PBE0/6-31+G(d)	ωB97x-D/6-31G(d)	SMD	593	624	31
	CAM-B3LYP/6-311+G(d,p)	CAM-B3LYP/6-31+G(d)	PCM	579	6159	37
6c	CAM-B3LYP/6-311+G(d,p)	ωB97x-D/6-31G(d)	SMD	596	631	35
	CAM-B3LYP/6-311+G(d,p)	**ωB97x-D/6-31G(d)**	**PCM**	**599**	**634**	**35**
	ωB97x-D /6-311+G(d,p)	ωB97x-D/6-31G(d)	SMD	5918	628	37
	B3LYP/6-311+G(d,p)	ωB97x-D/6-31G(d)	SMD	622	651	29
	PBE0/6-31+G(d)	ωB97x-D/6-31G(d)	SMD	611	640	29
	CAM-B3LYP/6-311+G(d,p)	CAM-B3LYP/6-31+G(d)	PCM	601	633	32

The ICT S_1 is unobtainable by direct excitation and requires a kinetic transition from the LE S_1[19e]. Due to its pseudo-zwitterionic properties, the ICT S_1 will possess significantly higher dipole moment than the ground state S_0 and LE S_1, causing it to be more stable in polar solvents. Both of these phenomena will result in the observation of the dual fluorescence in the UV spectra produced by the LE S_1 and ICT S_1 with the ICT fluorescence peak increasing in magnitude with the solvent polarity.

As dual fluorescence is absent in our squaraine dyes in both polar and non-polar solvents (Table 2 & 3), this rules out the ICT mechanism in triggering the large Stokes shift observed.

In organic fluorophores, local excitation mechanism can cause significant Stokes shift due to the resonance effects being more dominant in the excited state stabilization while steric hindrance is more prominent in the ground state stabilization. This hierarchical change of stabilization factors during excitation creates a substantial geometric change in the process. Liu and coworkers[20] exploited this feature in the local excitation mechanism by adding a rotatable substituent that can form conjugation with the fluorophore scaffold and customizing the steric hindrance on the substituent. The rotatable controlled steric hindrance on the substituent is strong enough to form a stabilized non-planar ground state structure but weak enough to be overridden by the mesomeric effect during the excited state formation to form a planar structure where the resonance is maximized to cause a substantial geometric change.

To understand the factors causing the large Stokes shift in **6a** in comparison to its structurally analogues **3a** and **6b** and **6c**, TDDFT calculations with implicit solvation in DMSO were utilized. CAM-B3LYP/6-311+G(d,p) TDDFT calculations with PCM[21] solvation in DMSO gave the best qualitative trend with the calculated Stokes shift for **3a** at 63 nm while that for **6a** was 79 nm (Table 2). Initially a benchmark TDDFT studies at the 6-311+G(d,p) level with long range corrected functionals (CAM-B3LYP[22], ωB97X-D[23] and LC-BLYP[24]) and popular DFT methods , B3LYP and PBE0 were computed with ωB97X-D/6-31G(d) optimized structures. SMD[25] implicit solvation in DMSO was included in both TDDFT and optimization calculations (Table 2). Only long range corrected functionals were able to correctly determine the larger Stokes shift of **3a** and **6a** compare to **6b** and **6c**, demonstrating the importance of range correction in TDDFT calculations. To eliminate the possibility of the results being an artifact of ωB97X-D/6-31G(d) geometries, CAM-B3LYP/6-311+G(d,p) TDDFT calculations were accomplished with CAM-B3LYP / 6-31+G(d) and PBE0/6-31+G(d) optimized structures to affirm that the qualitative trend of the Stoke shift (Table 2). The resulting Stokes shift reiterates the qualitative trend with respect to the experimental result.

The TDDFT calculations predicted that for **3a** and **6a, 6b** and **6c**, both the excitation (S0→S1) and fluorescence (S1→S0) is caused primarily by the HOMO to LUMO transition. The π conjugation is

predominant in the HOMO and LUMO of **3a**, **6a 6b** and **6c** and its excited states (Supporting Information Figure S1-S4), predicting that both the excitation and fluorescence involves a π to π* transition. The orbital contributions from the ketone and dicyanovinyl functional group on the squarate core (Figure 2) are absent in the LUMO while the squarate core has a significant contribution in the HOMO. This suggests that the squarate core have significant influence on the stabilization of the HOMO of the system. The involvement of the orbital of the dibutylamine N moiety in both the HOMO and LUMO suggest its significance in affecting both the S_0 and S_1 state in the LE mechanism.

The magnitude of the Stokes shift is a result of the magnitude of the geometric change between the absorption state and the fluorescence state geometry. The geometric and electron density change between the ground and excited state due to local excitation are studied to elucidate the factors behind the Stokes shift.

3a   **6a**

HOMO

LUMO

6b   **6c**
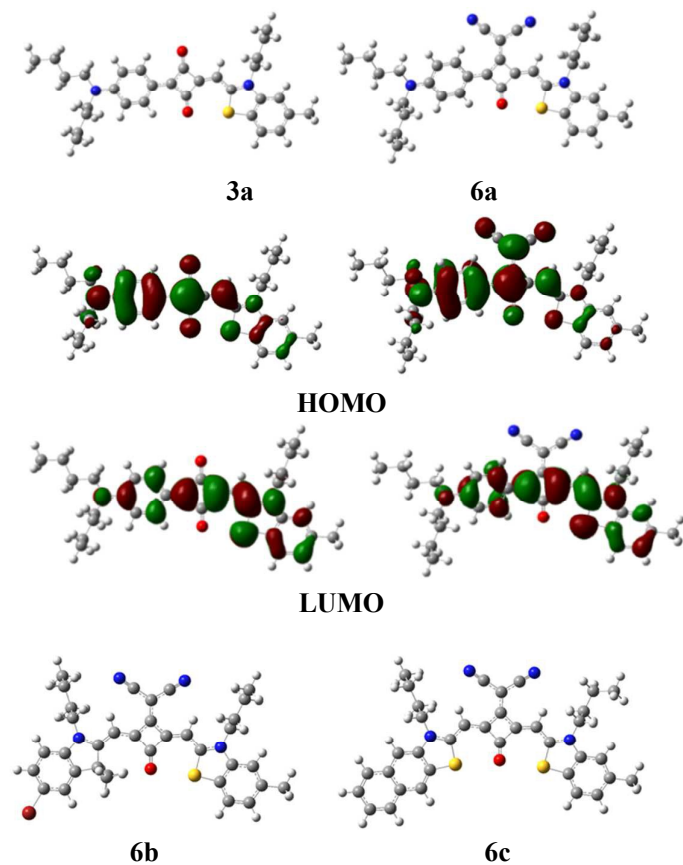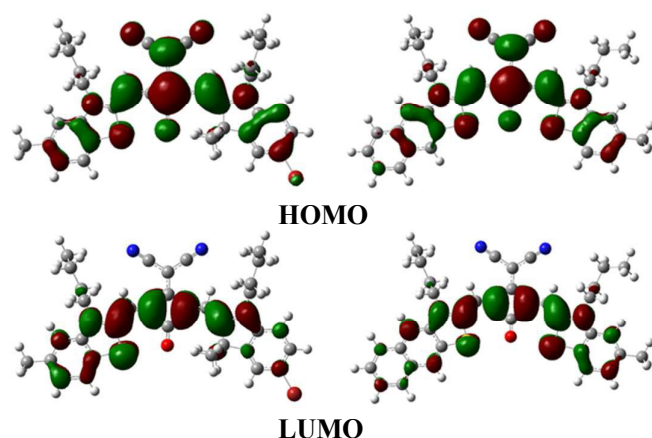
HOMO

LUMO

Figure 2. Isodensity plot of molecular orbitals (HOMO and LUMO) of **3a**, **6a, 6b** and **6c** at ground state.

The deviation from planarity of the ground and excited state is used to evaluate the geometric change and assess the degree of optimization of the resonance effect. The dihedral angle deviation from planarity in the S_0 and S_1 state (θ, Supporting information Table S2-S5) is taken to compare the mesomeric effects where the geometric change in reflected in their dihedral deviation difference ($\Delta\theta$, Table 4).The non-planarity of the dicyanovinyl functional group with respect to the squarate core and the phenyl ring of the N, N-dibutyl-aniline in **6a** S_0 caused the significant geometric change during excited state relaxation when mesomeric effects are maximized to form a near planar S_1 state (Table 4 and Figure 3). This is shown by the dihedral angle difference (θ_a, θ_{a2} and θ_b, Supporting Information Table S2-S5) of the mentioned functional group in S_0 and S_1 state. Despite the planarity of the π conjugated ring system in both **3a** S_0 and S_1 state ($\Delta\theta_b$), the significant Stokes shift is caused by the steric interaction between the N,N-dibutyl-amine functional group and the phenyl ring ($\Delta\theta_a$, $\Delta\theta_{a2}$). This impedes the mesomeric interaction of the amine with the phenyl ring and the π conjugated system in the ground state, preventing the amine from achieving a planar geometry. Both 6b and 6c S_0 and S_1 states have near planar geometries which do not experience much geometrical changes during excitation (Table 4) as shown in the small Stokes shift in Table 3.

Table 3. TDDFT results for squarine dyes 3a, 6a, 6b and 6c in DMSO, MeOH, CHCl$_3$ and Hexane.

CAM-B3LYP /6-311+G(d,p) was used for TDDFT calculations using   ωB97x-D/6-31G(d) structures.

PCM solvation was included in all calculations. The reorganization energies are given in kJmol^{-1}

Dyes	Solvent	λmax	λem	$\Delta\lambda_{cal}$	$\Delta\lambda_{exp}$	ΔE_{S1}^{Reorg}
3a	DMSO	519	582	63	65	13
	MeOH	515	575	60	61	12
	CHCl$_3$	536	585	49	38	10
	Hexane	546	585	40	15	7.4
6a	DMSO	528	606	78	**90**	**16**
	MeOH	525	600	75	80	15
	CHCl$_3$	557	617	60	67	12
	Hexane	580	631	51	26	9.3
6b	DMSO	578	616	38	32	6.1
	MeOH	574	609	35	31	5.9
	CHCl$_3$	594	628	34	26	5.6
	Hexane	605	628	33	10	5.5
6c	DMSO	599	634	35	27	5.3
	MeOH	593	626	33	25	5.3
	CHCl$_3$	615	648	33	28	5.1
	Hexane	627	640	13	16	5.3

Cave et al.[26] demonstrated that reorganization energy (Eq.1) of the ground and excited state can be used as a qualitative relationship between the geometrical and energetic changes. From Table 3, the trend of the increasing Stokes shift with the corresponding increase in reorganization energy of the S_1 state correlates with the respective magnitude of the geometrical change in Table 4.

The reorganization energy of the S_1 state is given by the equation

$$\Delta E_{S1}^{Reorg} = E_{S1}(X_{S0}) - E_{S1}(X_{S1}) \qquad (1)$$

where X_{S0} and X_{S1} represent the equilibrium geometries for the S_0 and S_1 states, respectively while $E_{S1}(X_{S0})$ and $E_{S1}(X_{S1})$ is defined as the energies for the S_1 state calculated at X_{S0} (absorption) and X_{S1},(fluorescent) process respectively.

To account for the difference in steric repulsion experience by the S_0 and S_1 state, the NCI analysis[27] is employed. The NCI index is based on a 2D plot of the reduced density gradient, s, and the electron density, ρ. The reduced density gradient, s, is derived from the electron density (ρ) of a system and its first derivative (Eq. 2).

$$s = \frac{1}{2(3\pi^2)^{\frac{1}{3}}} \frac{|\nabla \rho|}{\rho^{\frac{4}{3}}} \qquad (2)$$

To differentiate between attractive and repulsive non-covalent interactions, the sign of the Laplacian of the density, $\nabla^2\rho$ is used. The Laplacian is decomposed into a sum of contributions along the three principal axes of maximal variation. These components are the three eigenvalues λ_i of the electron-density Hessian (second derivative) matrix, such that $\nabla^2\rho = \lambda_1 + \lambda_2 + \lambda_3$, ($\lambda_1 < \lambda_2 < \lambda_3$). The second eigenvalue λ_2 is used to differentiate the attractiveness or repulsiveness of an interaction. A positive sign $\lambda_2 > 0$ (red isosurface) signifies steric repulsion while a negative sign $\lambda_2 < 0$, (green to beige isosurface) shows attractive non-covalent interactions such as Van der Waals or C-H-O interaction. This popular non covalent interaction evaluation method has been applied to both chemical and bio-system to analyse the essential intra and intermolecular interaction features.

The excited states of both **6a** (Figure 3) and **3a** (Supporting information Figure S6) experiences higher steric interactions compared to its ground state as there is an observed increase in the red isosurface. This is a result of the hierarchical change of resonance interaction overriding the steric interactions in the excited state for both 3a and 6a, generating a more planar structure that experience more steric repulsion but maximizes the mesomeric effect. The higher geometric change in **6a**.

An index described by Guido and coworkers, Δr[27] was introduced to characterize the amount of spatial rearrangement when the exchange correlation functional is inadequate to describe the charge transfer excitation. This is an issue for Tozer et al. Λ diagnostic index which in some cases is unable to differentiate the magnitude of short range charge transfer or local excitation. The hole−particle pair interactions using Δr is related to the average distance covered during the excitations correlated to the function of the excitation coefficients.

$$\Delta r = \frac{\sum_{ia} K_{ia}^2 |\langle \varphi_a|r|\varphi_a \rangle - \langle \varphi_i|r|\varphi_i \rangle|}{\sum_{ia} K_{ia}^2} \qquad (3)$$

where

$$K_{ia} = X_{ia} + Y_{ia} \qquad (4)$$

The composition of X_{ia} (excitation coefficient) and Y_{ia} (de-excitation coefficient) is made up of the molecular orbital overlap between the occupied orbitals φ_i and the virtual orbitals φ_a involved in the electronic transition.The Δr distance is related to the nature of the transition where the valence excitations and LE are characterized by short distances, while larger distances are associated with charge transfer excitation.

The Δr trend observed in Table 4 sees a higher CT characteristic in the excitation for both 3a and 6a with a larger Δr. This is consistent with the more significant geometrical change between the S_0 and S_1 in addition to the higher planarity of the excited structure where the optimized mesomeric interaction in S_1 will stabilize a more polarized moiety. The smaller Δr value for **6b** and **6c** show the strong LE character of the excitation. The lack of NCI isosurface change between the S_0 and S_1 state shows the absence of competing mesomeric and steric induced geometrical change.

Table 4.   The geometric change reflected in the dihedral angle difference between the S_0 and S_1 state's deviation from planarity ($\Delta\theta$) for squarine dyes 3a, 6a, 6b and 6c in DMSO, MeOH, CHCl$_3$ and Hexane. CAM-B3LYP /6-311+G(d,p) was used for TDDFT calculations using   ωB97x-D/6-

Dye	Solvent	$\Delta r/\text{Å}$ [a]	$\Delta\theta_a$ [b]	$\Delta\theta_{a2}$	$\Delta\theta_b$	$\Delta\theta_c$	$\Delta\theta_d$	$\Delta\theta_e$
3a	DMSO	1.34 [3.13]	4.1	8.8	0.0	0.1	0.5	1.3
	MeOH	1.35 [3.03]	4.7	8.1	0.1	0.1	0.5	0.7
	CHCl$_3$	1.51 [2.76]	3.1	7.9	0.1	0.1	0.4	0.5
	n-Hexane	1.66 [2.40]	1.8	6.2	0.3	0.5	0.6	0.3
6a	DMSO	1.33 [3.22]	2.6	7.1	14.5	5.3	3.2	0.3
	MeOH	1.34 [3.21]	2.5	7.1	14.4	5.3	3.1	0.3
	CHCl$_3$	1.55 [2.92]	4.8	3.2	6.5	3.9	0.8	0.3
	n-Hexane	1.76 [2.61]	2.3	1.9	2.0	1.9	0.1	0.7
6b	DMSO	0.63 [1.28]	0.2	-	2.8	0.3	0.6	1.6
	MeOH	0.64 [1.25]	0.4	-	0.9	0.5	0.3	1.0
	CHCl$_3$	0.75 [1.18]	0.2	-	0.6	0.3	0.5	0.7
	n-Hexane	0.89 [1.10]	0.2	-	0.1	0.3	0.5	0.4
6c	DMSO	0.69 [0.92]	0.1	-	4.5	1.4	0.2	1.8
	MeOH	0.71 [0.86]	0.1	-	1.5	1.3	0.1	1.8

.31G(d) structures. PCM solvation was included in all calculations.

CHCl₃	0.78 [0.85]	0.2	-	1.5	1.3	0.2	1.4
n-Hexane	0.90 [0.90]	0.2	-	1.5	1.3	0.8	0.9

3a　　6a

6b　　6c
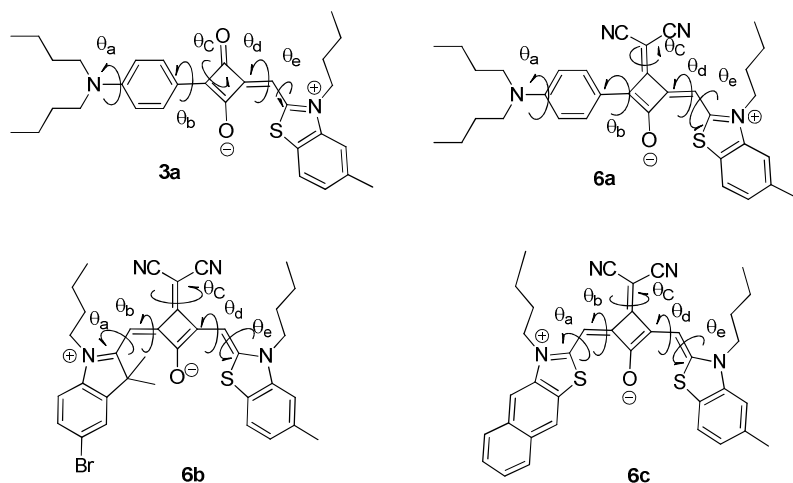
[a] The value of Δr in parenthesis refers to that of the S_0 while the other value refers to that of the excited state. [b] $\Delta\theta$ is the dihedral angle between the S_0 and S_1 state's deviation from planarity. θ is calculated as the dihedral angle deviation from planarity where the values are taken form the modulus the difference of dihedral angle from 180° or 0° (i.e. 180°-|x| if x > 90° or |x|-0 if x < =90°), whichever is nearer to attaining a planar structure. The dihedral angles taken are shown in the figure to the left and also listed by its atomic label below its value in Table S2. Only for **3a** and **6a** will $\Delta\theta a_2$ be applicable as it measures the dihedral angle of both t-butyl groups with respect to the phenyl ring.
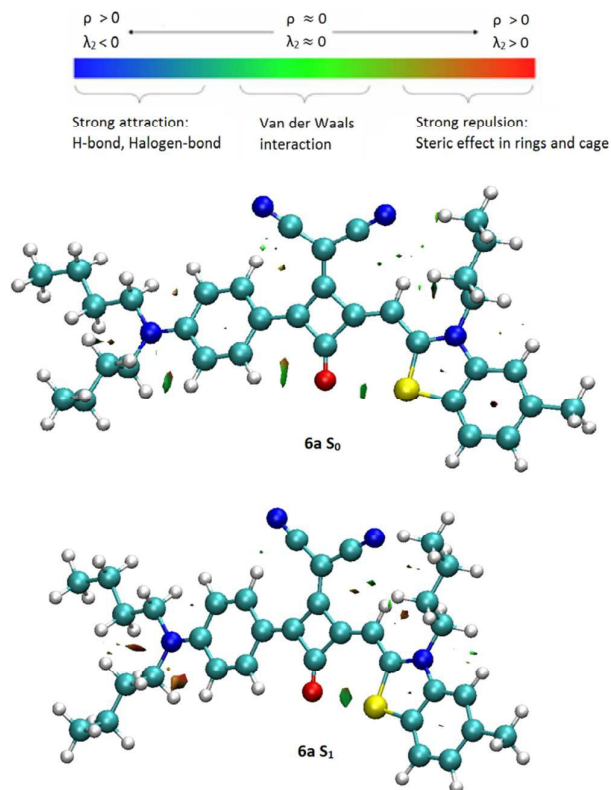
Figure 3. **6a** S_0 and S_1 RDG isosurface. Steric repulsion (red isosurface) between the N,N-butyl groups with the phenyl ring is increased significantly in the excited state as mesomeric effects override the steric influence.

The solvent effects are reflected in Table 3 where the decrease in the solvent polarity by comparing DMSO to chloroform and to hexane results in the corresponding decrease in Stokes shift. This is caused by the decreasing stabilization of a more polarized and planar geometry in the excited state. This phenomenon is demonstrated in the increase of θ (Supporting information, Table Sx) for all the squarine dyes S_1 states in $CHCl_3$ and n-Hexane solvents where they are unable to attain the more planar structure as achieved in the polar solvent DMSO. This result in a smaller geometric change between the solvated and excited state (Δθ, Table 4), hence a smaller Stokes shift (Table 3).

3. Conclusion

To conclude, six asymmetric squaraines were synthesized in a multistep manner through two semi-squaraine salts. Such an amenable strategy facilitates: (1) high value asymmetrical squaraines; (2) independent structure optimization to tune absorption and emission wavelengths within range from 600 nm to 720 nm. The quantum yields of these dyes are comparable to commercial available cyanine dyes. The unique large stokes shifts (up to 90 nm) are observed for this series of squaraines (especially for **6a**) which can offer direct applications in multichannel molecular imaging with a clear and readable signal. TDDFT calculations indicate that the steric effect from N,N-dibutyl groups with the phenyl ring and the dicyanovinyl group on the squarate core contributes to the large geometric change, resulting in the large Stokes shift. All these findings help us to understand the relationships between structures and physical properties of squaraines.

Computational Details

All TDDT calculations were run in Gaussian 09 Rev B.01 [31] and molecular orbitals and electron density analysis were computed with Multiwfn. [32]

Experimental Section

Materials and methods, details of synthesis and characterization of final compounds and all spectrums of absorption and emission for these dyes have been listed in the supporting information.

Conflict of interest

The authors declare no competing financial interest.

Acknowledgements

References

1   (a) M. Panigrahi, S. Dash, S. Patel and B. K. Mishra, *Tetrahedron*, **2012**, 68, 781; (b) K. Y. Law, Chem. Rev., **1993**, 93, 449; (c) A. Ajayaghosh, *Acc. Chem. Res*., **2005**, 38, 449;

(d) W. Shi and H. Ma, *Chem. Comm*, **2012**, 48, 8732; (e) J. J. McEwen and K. J. Wallace, *Chem. Comm*. **2009**, 6339; (f) S. L. Lam, X. Liu, F. Zhao, C. L. K. Lee and W. L. Kwan, *Chem. Comm*, **2013**, 49, 4543; (g) F. Silvertri, M. D. Irwin, L. Beverina, A. Facchetti, G. A. Pagani and T. J. Marks, *J. Am . Chem. Soc*, **2008**, 130, 17640; (h) J. H. Yum, P. Waltre, S. Huber, D. Rentsch, T. Geiger, F. Nuesch, F. D. Angelis, M. Gratzel and M. K. Nazeeruddin, *J. Am. Chem. Soc*, **2007**, 129, 10320; (i) D. Demeter, T. Rousseau, P. Leriche, T. Cauchy, R. Po and J. Roncali, *Adv. Funct. Mater*. **2011**, 21, 4379.

2 (a) B. Oswald, L. Patsenker, J. Duschl, H. Szmacinski, O. S. Wolfbeis and E. Terpetschnig, *Bioconjugate Chem*., **1999**, 10, 925; (b) B. Oswald, M. Gruber, M. Bohmer, F. Lehman, M. Probst and O. S. Wolfbeis, *Photochem. Photobiol.,* **2001**, 74, 237; (c) L. D. Patsenker, A. L. Tatarets, Ye. A. Povrozin and E. A. Terpetschnig, *Bioanal. Rev*., **2011**, 3, 115; (d) J. J. Lee, A. G. White, J. M. Baumes and B. D. Smith, *Chem. Commun*. **2010**, 46, 1068; (e) E. M. Sevick-Muraca, J. P. Houston and M. Gurfinkel, *Curr. Opin. Chem. Biol.*, **2002**, 6, 642; (f) M. S. Goncalves, *Chem. Rev*., **2009**, 109, 190; (g) R. R. Avirah, D. T. Jayaram, N. Adarsh and D. Ramaiah, *Org. Biomol. Chem*., **2012**, 10, 911; (h) J. M. Baumes, J. J. Gassensmith, J. Giblin, J. J. Lee, A. G. White, W. J. Culligan, W. Leevy, M. Kuno and B. D. Smith, *Nat. Chem*., 2010, 2, 1025; (i) K. Funabiki, H. Mase, Y. Saito, A. Otsuka, A. Hibino, N. Tanaka, H. Miura, Y. Himori, T. Yoshida, Y. Kubota, and M. Matsui, *Org Lett.*, **2012**, 14, 1246.

3 (a) Y. Y. Huang, P. Mroz, T. Zhiyentayev, S. K. Sharma,T. Balasubramanian, C. Ruzie, M. Krayer, D. Fan, K. E. Borbas, E. Yang, H. L. Kee, C. Kirmaier, J. R. Diers, D. F. Bocian, D. Holten, J. S. Lindsey and M. R. Hamblin, *J. Med. Chem*., **2010**, 53, 4018; (b) S. H. Lim, C. Thivierge, P. N. Sliwinska, J. Y. Han, H. V. D. Bergh, G. Wagnières, K. Burgess and H. B. Lee, *J. Med. Chem.,* **2010**, 53, 2865; (c) V. Rapozzi,L. Beverina, P. Salice, G. A. Pagani, M. Camerin and L. E. Xodo, *J. Med. Chem.,* **2010**, 53, 2188; (d) M. Obata, S. Hirohara, R. Tanaka, I. Kinoshita, K. Ohkubo, S. Fukuzumi, M. Tanihara and S. Yano, *J. Med. Chem.,* **2009**, 52, 2747; (e) T. Lu, P. Shao, I. Mathew, A. Sand and W.

Sun, *J. Am. Chem. Soc.*, **2008**, 130, 15782; (f) P. K. Frederiksen, S. P. McIlroy, C. B. Nielsen, L. Nikolajsen, E. Skovsen, M. Jørgensen, K. V. Mikkelsen and P. R. Ogilby, *J. Am. Chem. Soc.*, **2005**, 127, 255; (g) A. Gorman, J. Killoran, C. O'Shea, T. Kenna, W. M. Gallagher and D. F. O'Shea, *J. Am. Chem. Soc.*, **2004**, 126, 10619; (h) M. R. Detty, S. L. Gibson and S. J. Wagner, *J. Med. Chem.*, **2004**, 47, 3897. (i) H. S. Choi, K. Nasr, S. Alyabyev, D. Feith, J. H. Lee, S. H. Kim, Y. Ashitate, H. Hyun, G. Patonay, L. Strekowski, M. Henary and J. V. Frangioni, *Angew. Chem. Int. Ed,.* **2011**, 50, 6258; (j) Y. Xu, B. Li, P. Han, S. Sun and Y. Pang, *Analyst*, **2013**, 138, 1004; (k) K. M. Shafeekh, S. Das, C. Sissa, A. Painelli, *J Phys. Chem B.,* **2013**, 117, 8536.

4   (a) P. G. Jönsson and Å. Kvick, *Acta Cryst.B.*, **1972**, 28, 1827; (b) P. D. William; R. A. Jockusch, R. E. Williams, *J. Am. Chem. Soc.* **1997**, 119, 11988; (c) H. S. Choi, K. Nasr, S. Alyabyev, D. Feith, J.H. Lee, S. H. Kim, Y. Ashitate, H. Hyun, G. Patonay, L. Strekowski, M. Henary and J. V. Frangioni, *Angew. Chem. Int. Ed.* **2011**, 6258; (d) W. Liu, H. S. Choi, J. P. Zimmer, E. Tanaka, J. V. Frangioni, M. Bawendi, *J. Am. Chem. Soc.* **2007**, 129, 14530; (e) H. S. Choi, J. V. Frangioni, *Mol. Imaging.* **2010**, 9, 291.

5   (a) C. Luo, Q. Zhou, B. Zhang and X. Wang, *New J. Chem.*, **2011**, 35, 45; (b) L. Beverina and P. Salice, *Eur. J. Org. Chem.,* 2010; (c) A. Ajayaghosh, *Acc. Chem. Res.*, **2005**, 38, 449; (d) A. Ajayaghosh, *Chem. Soc. Rev.*, **2003**, 32, 181. (e) M. V. Reddington, *Bioconjugate Chem.* **2007**, 8, 2178; (f) V. Rapozzi, L. Beverina, P. Salice, G. A. Pagani, M. Camerin and I. E. Xodo, *J. Med. Chem.* **2010**, 53, 2188; (g) U. Mayerhoffer, M. Gasanger, M. Stolte, B. Fimmel and F. Wurthner, *Chem. Eur. J.* **2013**, 19, 218; (h) U. Mayerhoffer, B. Fimmel and F. Wurthner, *Angew. Chem. Int. Ed.* **2012**, 51, 164.

6   (a) J. Y. Li, C. Y. Chen, C. P. Lee, S. C. Chen, T. H. Lin, H. H. Tsai, K. C. Ho, C. G. Wu, *Org. Lett*, **2010**, 12, 5454; (b) L. Beverina, R. Ruffo, M. M. Salamone, E. Ronchi, M. Binda, D. Natali, M. Sampietro, *J. Mater. Chem.* **2012**, 22, 6704.

7   (a) Y. Q. Liu, A. Malkovskiy, Q. M. Wang, Y. Pang, *Org. Biomol. Chem*, **2011**, 9, 2878. (b) L. I. Markova, V. L. Malinovskii, L. D. Patsenker, R. Haner, *Org. Biomol. Chem*, **2012**, 10, 8944.

8   (a) D. Keil and H. Hartmann, *Dyes Pigm*., **2001**, 49, 161; (b) S. Sreejith, P. Carol and A. Ajayaghosh, *J. Mater. Chem.* **2008**, 18, 264; (c) J. Chen and R. F. Winter, *Chem. Eur. J,* **2012**, 18, 10733; (d) D. E. lynth, A. N. Kirkham, M. Chowdhury, E. S. Wane and J. Heptinstall, *Dyes and Pigm*, **2012**, 94, 393; (e) Y. Shi, R. B. Hill, J. H. Yum, A. Dualeh, S. Barlow, M. Gratzel, S. R. Marder and M. K. Nazeeruddin, *Angew. Chem. Int. Ed*, **2011**, 50, 6619.

9   (a) S. S. Pandey, R. Watanable, N. Fujikawa, G. M. Shivashimpi, Y. Ogomi, Y. Yamaguchi, S. Hayase, *Tetrahedron,* **2013**, 69, 2633; (b) S. Kuster, T. Geiger, *Dyes and Pigm*, **2012**, 657.

10 (a) M. C. Basheer, U. Santhosh, S. Alex, K. G. Thomas, C. H. Suresh and S. Das, *Tetrahedron*, **2007**, 63, 1617.

11 (a) S. Kim, G. K. Mor, M. Paulose, O. K. Varghese, C. Baik, C. A. Grimes, *Langmuir*, **2010**, 26, 13486; (b) V. Hrobarikova, p. Hrobarik, P. Gajdos, I. Fitilis, M. Fakis, P. Persephonis, P. zahradnik, *J. Org. Chem*., **2010**, 75, 3053.

12 (a) S. Yasui, M. Matsuoka, T. Kitao, *Dyes Pigm*., **1988**, 10, 13; (b) Z-S. Wang, F. Y. Li, C. H. Huang, *J. Phys. Chem. B*. **2001**, 105, 9210.

13 (a) Law, K.-Y. *Chem. Rev.* **1993**, 93, 449; (b) Bello, K. A.; Corns, S. N.; Griffiths, *J. Chem. Soc., Chem. Commun*., **1993**, 452; (c) Sprenger, H. E.; Ziegenbein, W. *Angew. Chem., Int. Ed. Engl.* **1966**, 5, 893.

14 (a) L. H. Liu, K. Nakatani, R. Pansu, J. J. Vachon, P. Tauc, E. Ishow, *Adv. Mater*., **2007**, 19, 433; (b) V. Ramalingam, M. E. Domaradzki, S. Jang, R. S. Muthyala, *Org. Lett.,* **2008**, 15, 3315.

15 (a) Y. Shi, R. B. Hill, J. H. Yum, A. Dualeh, S. Barlow, M. Gratzel, S.R. Marder, M. K. Nazeerudin, *Angew. Chem. Int. Ed,* **2011**, 50, 6619; (b) C. H. Chang, Y.C. Chen, C.Y. Hsu, H. H. Chou, J. T. Lin, *Org. Lett*, **2012**, 14, 4726; (c) J. Chen, R. F. Winter, *Chem. Eur. J.* **2012**, 18, 10733; (d) S. Kuster, T. Geiger, *Dyes and Pigments*, **2012**, 95, 657.

16 (a) U. Mayerhoffer, M. Gsanger, M. Stolte, B. Fimmel, F. Wurthner, *Chem. Eur. J.*, **2013**, 19, 218; (b) S. Kim, G. K. Mor, M. Paulose, O. K. Varghese, C. Baik, C. A. Grimes, *Langmuir*, **2010**, 26, 13486.

17 M. Klessinger, *Chem. Unserer Zeit*, **1978**, 12, 1.

18 (a) I. Gómez, M. Reguero, M. Boggio-Pasqua, M. A. Robb, *J. Am. Chem. Soc.* **2005**, 127, 7119; (b) K. Rotkiewicz, K. H. Grellmann, Z. R. Grabowski, *Chem Phys Lett,* **1973**, 21, 212; (c) K. A. Zachariasse, S. I. Druzhinin, W. Bosch, R. Machinek, *J. Am. Chem. Soc.* **2004**, 126, 1705; (d) A.-D. Gorse, M. Pesquer, *J. Phys. Chem.* **1995**, 99, 4039; (e) W. Schuddeboom, S. A. Jonker, J. M. Warman, *J. Phys. Chem.* **1992**, 96*,* 10809.

19 X. Liu, Z. Xu, J. M. Cole, *J. Phys. Chem. C*, **2013**, 117, 16584.

20 S. Miertus, E. Scrocco, J. Tomasi, *Chem. Phys.* **1981**, 55, 117.

21 T. Yanai, D. Tew, N. Handy, *Chem. Phys. Lett.*, **2004**, 393, 51.

22 J. D. Chai, M. Head-Gordon, *Phys. Chem. Chem. Phys.,* **2008**, 10, 6615.

23 H. Iikura, T. Tsuneda, T. Yanai, K. Hirao, *J. Chem. Phys.*, **2001**, 115, 3540.

24 A. V. Marenich, C. J. Cramer, D. G. Truhlar, *J. Phys. Chem. B*, **2009**, 113, 6378.

25 (a) E. R. Johnson, S. Keinan, P. Mori-Sanchez, J. Contreras-Garcia, A. J. Cohen, W. Yang, *J. Am. Chem. Soc.* **2010**, 132, 6498; (b) J. Contreras-Garcia, E. R. Johnson, S. Keinan, R. Chaudret, J-P. Piquemal, D. N. Beratan, W. Yang, *J. Chem. Theory Comput.* **2011**, 7, 625; (c) J. M. V. Franco, A. E. Ferao, G. Schnakenburg, R. Streubel, *Chem. Commun.,* **2013**, 49, 9648.

26 R. J. Cave, K. Burke, E. W. Castner Jr., *J. Phys. Chem. A* **2002,** *106,* 9294.

27 C. A. Guido, P. Cortona, B. Mennucci, C. Adamo, *J. Chem. Theory Comput.* **2013**, 9, 3118.